

HUMAN-LIKE MOTION FROM PHYSIOLOGICALLY-BASED POTENTIAL ENERGIES

O. Khatib, J. Warren, V. De Sapio, L. Sentis

Robotics Laboratory, Department of Computer Science

Stanford University, Stanford, California 94305

{khatib, warren, vdesap, lsentis}@robotics.stanford.edu

Abstract Generating coordinated natural motion in human-like robotic structures has proved to be a challenging task. Given that humans easily solve this problem, we propose a methodology to devise the underlying strategies of human movement and apply them for robotic control. We use this approach to examine how humans utilize their muscles while performing positioning tasks. This analysis suggests an effort potential that is shown to characterize human postural motion. By applying this methodology to other criteria, we seek to establish a basis of human motion characteristics.

Keywords: human motion behaviors, task-level control, muscle kinematics and dynamics, task/posture decomposition

1. Introduction

The challenge of synthesizing motion behaviors is a long-standing problem within the robotics community. With the recent advent of complex humanoid systems, this challenge grows ever demanding. Due to their anthropomorphic design, humanoids should move in a human-like manner to facilitate movement within man-made environments and to promote interaction with their biological counterparts. Common strategies involve generating joint space trajectories (Kuroki, 2003) or learning specific motions (Ijspeert, 2002), but these approaches require off-line computations and do not generalize well to related tasks. There is a pressing need for a framework where natural motion is generated in real-time for a large range of tasks.

From observations of human motion, it is apparent that people perform many different behaviors while executing a task. These secondary criteria are the essence of natural human motion, affecting not *whether* but *how* the task is achieved. Fig. 1 contrasts poses of two humanoids performing a hands positioning task. By simultaneously controlling the balance and maximizing mobility, the left humanoid visibly exhibits a more human-like behavior. With this as motivation, we have developed



Figure 1. Comparison of configurations while performing a hand positioning task. By maintaining balance and maximizing mobility, the left humanoid has a markedly more natural posture than the one on the right.

a prioritized multiple task controller that in real-time dynamically decouples each task.

Equipped with this control framework, we propose a general methodology to discover the innate subtasks of human motion. These behaviors are initially identified by hypothesis or direct observation. By designing targeted motion capture experiments that excite these behaviors, we then confirm or refute their presence and ascertain their importance relative to other tasks. After identification, these behaviors are then incorporated into our robotic controller, incrementally creating a basis of tasks that characterize human-like movement.

We will illustrate this methodology by examining the muscular effort required to perform positioning tasks. In general terms, it is evident that humans avoid overexertion in commonplace motions. However, this concept is not easily quantified, nor is it clear of its relative importance to other behaviors. By utilizing biomechanical models for neuromuscular dynamics and control (Zajac, 1993; Hogan, 1991), we demonstrate that humans seek to minimize the muscular effort (normalized by torque capacity) needed to compensate for gravity while performing positioning tasks. While there are additional behaviors that characterize human motion, humans use much of the available redundancy for gravity effort minimization.

2. Prioritized Task-Level Control Framework

For any human movement, a person satisfies various criteria while performing the task at hand. These tasks have different priorities - maintaining balance is typically more vital than minimizing the required

effort - but all are addressed subject to this hierarchy. With this model in mind, we have previously developed a task-level control framework that performs multiple behaviors in a prioritized manner (Khatib, 2004).

To illustrate this framework, we examine the scenario involving two tasks. We begin by describing the dynamics of the robot in terms of its joints coordinates, \mathbf{q} ,

$$\mathbf{A}(\mathbf{q})\ddot{\mathbf{q}} + \mathbf{b}(\mathbf{q}, \dot{\mathbf{q}}) + \mathbf{g}(\mathbf{q}) = \mathbf{\Gamma} \quad (1)$$

For this system of n equations, $\mathbf{\Gamma}$ is the set of generalized joint torques, $\mathbf{A}(\mathbf{q})$ is the inertia matrix, $\mathbf{b}(\mathbf{q}, \dot{\mathbf{q}})$ represents the centrifugal and Coriolis forces and $\mathbf{g}(\mathbf{q})$ is the gravity effect.

We denote the m parameters of the primary task as \mathbf{x}_t , with $\mathbf{J}_t(\mathbf{q})$ representing its joint space Jacobian. The operational space framework (Khatib, 1987) first introduced the dynamically consistent inverse of the Jacobian,

$$\bar{\mathbf{J}}_t = \mathbf{A}^{-1} \mathbf{J}_t^T [\mathbf{J}_t \mathbf{A}^{-1} \mathbf{J}_t^T]^{-1} \quad (2)$$

and demonstrated that its use provides a task dynamic behavior model. More explicitly, $\bar{\mathbf{J}}_t^T$ projects the joint space dynamics (Eq. 1) into task space,

$$\bar{\mathbf{J}}_t^T [\mathbf{A}\ddot{\mathbf{q}} + \mathbf{b} + \mathbf{g} = \mathbf{\Gamma}] \implies \mathbf{\Lambda}_t \ddot{\mathbf{x}}_t + \boldsymbol{\mu}_t + \mathbf{p}_t = \mathbf{F}_t \quad (3)$$

In this space, $\mathbf{\Lambda}_t$ is the $m \times m$ task inertia matrix, and $\boldsymbol{\mu}_t$, \mathbf{p}_t , and \mathbf{F}_t are respectively the centrifugal and Coriolis forces, gravity effect, and generalized force.

By the principle of virtual work, forces in the task space, \mathbf{F}_t , are transformed into a joint torque, $\mathbf{\Gamma}_{\text{task}}$, by the relationship,

$$\mathbf{\Gamma}_{\text{task}} = \mathbf{J}_t^T \mathbf{F}_t \quad (4)$$

This torque/force relationship allows for the decomposition of the total torque into two dynamically decoupled vectors: the torque controlling the task behavior of \mathbf{x}_t and a torque that does not affect the task but controls the robotic posture (Khatib, 1995),

$$\mathbf{\Gamma} = \mathbf{\Gamma}_{\text{task}} + \mathbf{\Gamma}_{\text{posture}} \quad (5)$$

Torques are projected into the posture space by the operator,

$$\mathbf{N}_t^T = [\mathbf{I} - \mathbf{J}_t^T \bar{\mathbf{J}}_t^T] \quad (6)$$

and it is within this space that we will address our secondary task.

Since it will be controlled within the posture space of the primary task, we choose \mathbf{x}_p to denote the coordinates of the subtask and \mathbf{J}_p as

its Jacobian. The task-consistent posture Jacobian was introduced to incorporate the constraints of \mathbf{x}_t (Khatib, 2004),

$$\mathbf{J}_{p|t} = \mathbf{J}_p \mathbf{N}_t \quad (7)$$

The subtask may not be achievable if it conflicts with the primary task, but this Jacobian identifies the controllable directions. Moreover, the task-consistent posture Jacobian provides the dynamic behavior model of the subtask in this posture space,

$$\bar{\mathbf{J}}_{p|t}^T [\mathbf{A}\ddot{\mathbf{q}} + \mathbf{b} + \mathbf{g} = \mathbf{\Gamma}] \implies \mathbf{\Lambda}_{p|t} \ddot{\mathbf{x}}_{p|t} + \boldsymbol{\mu}_{p|t} + \mathbf{p}_{p|t} = \mathbf{F}_{p|t} \quad (8)$$

and the force/torque relationship,

$$\mathbf{\Gamma}_{\text{posture}} = \mathbf{J}_{p|t}^T \mathbf{F}_{p|t} \quad (9)$$

With these dynamic behavior models we can formulate a dynamically decoupled control to perform both tasks. For each task, we have a desired unit inertial behavior $\ddot{\mathbf{x}}_t = \mathbf{F}_t^*$ and $\ddot{\mathbf{x}}_p = \mathbf{F}_p^*$. To compensate for the dynamics within their respective spaces, we select control forces \mathbf{F}_t and $\mathbf{F}_{p|t}$ by,

$$\begin{aligned} \mathbf{F}_t &= \hat{\mathbf{\Lambda}}_t \mathbf{F}_t^* + \hat{\boldsymbol{\mu}}_t + \hat{\mathbf{p}}_t \\ \mathbf{F}_{p|t} &= \hat{\mathbf{\Lambda}}_{p|t} \mathbf{F}_{p|t}^* + \hat{\boldsymbol{\mu}}_{p|t} + \hat{\mathbf{p}}_{p|t} \end{aligned} \quad (10)$$

where $\hat{\cdot}$ denotes the estimates of the components of the dynamic models. (The modification $\mathbf{F}_{p|t}^* = \mathbf{F}_p^* - \ddot{\mathbf{x}}_{p|t}$ is needed since $\mathbf{\Gamma}_{\text{task}}$ induces a bias acceleration on \mathbf{x}_p .) Using the task/posture decomposition of torque and the force/torque relationships, the resulting control torque $\mathbf{\Gamma}$ is determined by,

$$\mathbf{\Gamma} = \mathbf{\Gamma}_{\text{task}} + \mathbf{\Gamma}_{\text{posture}} = \mathbf{J}_t^T \mathbf{F}_t + \mathbf{J}_{p|t}^T \mathbf{F}_{p|t} \quad (11)$$

This control framework allows for a conceptual partitioning of motion. The task can be controlled by a task field U_t that determines the desired behavior by its gradient: $\mathbf{F}_t^* = -\nabla_{\mathbf{x}_t} U_t$. In a similar manner, the posture behavior \mathbf{F}_p^* can be specified by a separate posture field U_p . We can therefore incorporate human motion behaviors by expressing these strategies as energy potentials. In the following sections we examine how humans address muscular effort and construct a posture field to capture this behavior.

3. Human Model

To examine muscular effort within the prioritized task control framework we have constructed a musculoskeletal model in conjunction with a

dynamic simulation environment. The SAI environment (Khatib, 2002) uses an $\mathcal{O}(n)$ recursive algorithm for computing the dynamics and control of an n -joint branching, articulated robotic mechanism.

Our human model consists of 25 joints and 144 musculo-tendon actuators (Fig. 2). The musculoskeletal data used in this model has been derived from SIMM models (Delp and Loan, 1995). The skeleton is modelled as a multibody system within SAI and each musculo-tendon unit is modelled using a three element Hill-type model (Schutte, 1992). In this model all musculo-tendon lengths, \mathbf{l} , can be uniquely determined from the skeletal configuration. From kinematics, differential changes in \mathbf{l} are given by $d\mathbf{l} = \mathbf{L} d\mathbf{q}$, where $\mathbf{L}(\mathbf{q})$ is the muscle Jacobian. From the principle of virtual work we conclude,

$$\mathbf{\Gamma} = \mathbf{L}^T \mathbf{f} \quad (12)$$

where \mathbf{f} is the vector of net musculo-tendon forces (with an appropriate sign convention adopted).

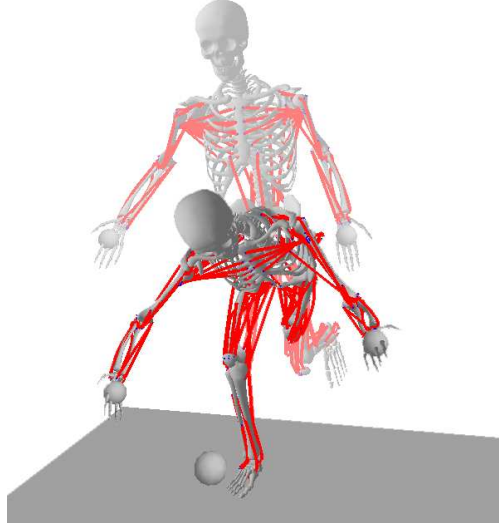


Figure 2. A human musculoskeletal model simulated in the SAI environment. This model consists of 25 joints and 144 musculo-tendon actuators.

The contraction dynamics of each musculo-tendon unit is modelled as depicted in Fig. 3a. The force-length-velocity relationship of the muscle at full activation is depicted in Fig. 3b. The active force component of this surface linearly scales by activation ($a \in [0, 1]$).

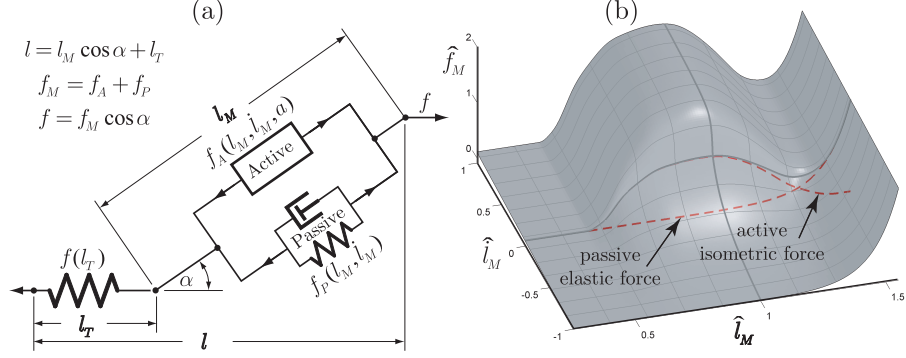


Figure 3. (a). Muscle model consisting of a parallel-series arrangement of active and passive elements. (b). Force-length-velocity relationship showing normalized muscle force, \hat{f}_M , as a function of muscle length, \hat{l}_M , and rate of contraction, $\hat{\dot{l}}_M$.

This overall model can be simplified if we take the tendon to be infinitely stiff. In this case the musculo-tendon force, f , can be computed as a function of \mathbf{q} , $\dot{\mathbf{q}}$, and a . From this we can compute feasible ranges for the tendon forces (between zero and full activation). Using Eq. 12, in conjunction with the feasible ranges of tendon forces, muscle induced torque boundaries, Γ_B , can be determined.

4. Muscular Effort Induced Postures

With the premise that musculoskeletal physiology plays an important role in the nature of human motion, we conducted preliminary exper-

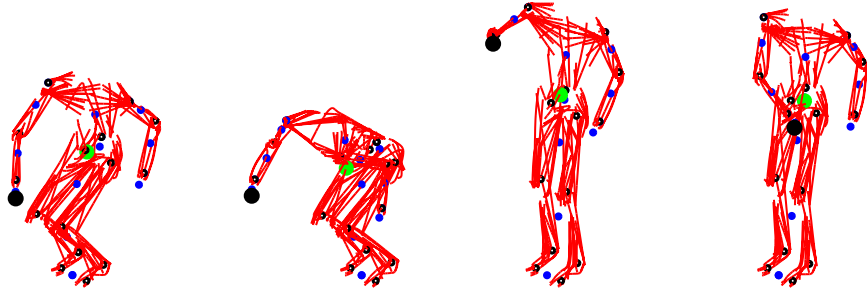


Figure 4. Captured skeletal configurations associated with a subject reaching to four different target locations with weight in hand. Muscle paths were overlaid based on the muscle model.

iments to investigate the manner in which humans address muscular effort while performing tasks. Three subjects were tracked using a motion capture system while performing whole-body reaching movements. This set of tasks required the subject to move a normalized weight to visual goal locations while keeping both feet grounded. Upon reaching a goal location, the subject maintained this task for 5 seconds while adjusting his posture to minimize discomfort. Fig. 4 depicts frames from the motion capture of a subject moving to separate target locations. Computational muscle models were used to overlay muscle paths over the configuration data.

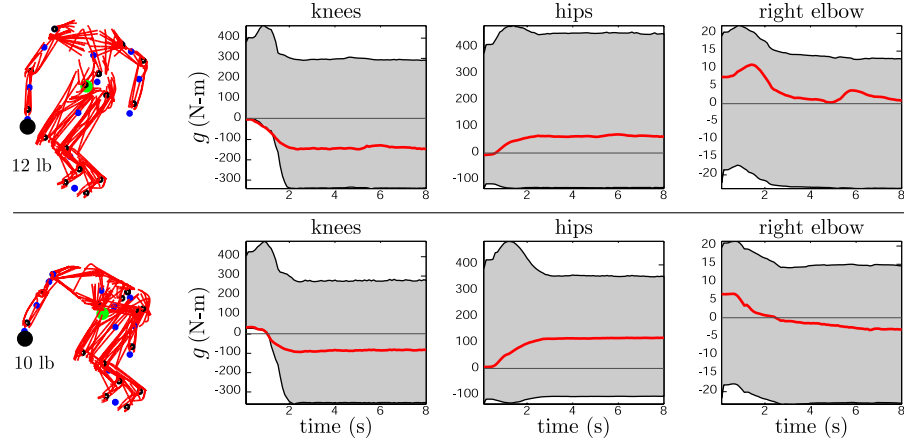


Figure 5. Captured skeletal configurations for reaching tasks, with selected gravity compensation torques shown. Boundaries represent muscle induced torque capacities.

From the joint space trajectories and our musculoskeletal model we can determine the muscular effort required to compensate for gravity. Fig. 5 shows samples of the processed data for two tests. We observe a strong trend that the gravity torques are balanced over the various joints in a manner that is correlated to the available torque capacity at each joint. Based on these observations, and past use of muscle-level weighted norm criteria in the biomechanics community (Anderson, 2001; Crowninshield, 1981), we conjecture that postural motion involves the minimization of a muscle effort potential, $U(\mathbf{q})$, of the form,

$$U(\mathbf{q}) = \sum_{i=1}^n w_i \frac{g_i(\mathbf{q})^2}{\Gamma_{B_i}(\mathbf{q})^2} \quad (13)$$

where g_i is the gravity torque about joint i , Γ_{B_i} is the muscle induced boundary torque (upper or lower boundary depending on the sign of g_i), and w_i is a weighting term.

We analyzed the suitability of the muscle effort potential in predicting quasi-static postures. Fig. 6 shows muscle effort computed over null space motion of arm configuration. A one dimensional null space was chosen for illustrative purposes. The variable q_p spans the task consistent manifold in configuration space (self motion manifold) and, in this case, represents the inclination angle of the plane of the arm. The configuration \mathbf{q}_{p_o} is the observed steady state configuration from the experimental data (third configuration in Fig. 4). This observed configuration is 0.13 radians (7.5°) from the configuration where the computed minimum occurs. The muscle effort computed at the observed configuration exceeds the minimum computed muscle effort by 1.6%.

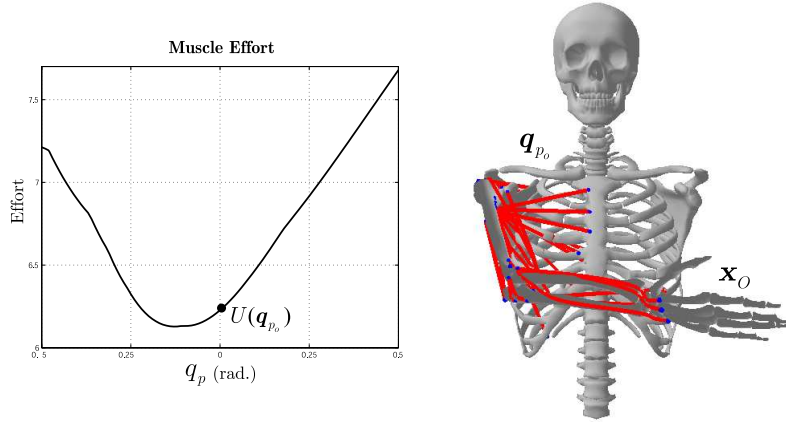


Figure 6. Plot showing muscle effort over null-space motion of arm configuration. Observed configuration, \mathbf{q}_{p_o} , is 0.13 radians (7.5°) from the configuration where the computed minimum occurs.

We also computed muscle effort over null space motion in whole body configuration. This is shown in Fig. 7. In addition to a task point at the right hand, \mathbf{x}_O , balancing was imposed with a task point at the center of mass of the system, \mathbf{x}_{cm} . Joints above the chest were locked to limit the dimension of the null space to one. The observed steady state configuration (second configuration in Fig. 4) is 0.27 radians (15.5°) from the configuration where the computed minimum occurs. The muscle effort computed at the observed configuration exceeds the minimum computed muscle effort by 3.6%.

For both the arm and whole body, uniform weighting was applied in computing the muscle effort. The efforts computed at the observed configurations exceed the minimum computed muscle efforts by less than 4%. This suggests strong correlation between task consistent human postures and a muscular effort criteria. While there are a number of sources of variability, including experimental error, model inaccuracies, and intrinsic variability in human motion (e.g. motion deadband); the results suggest a robust relationship between human motion and task-level muscular effort minimization.

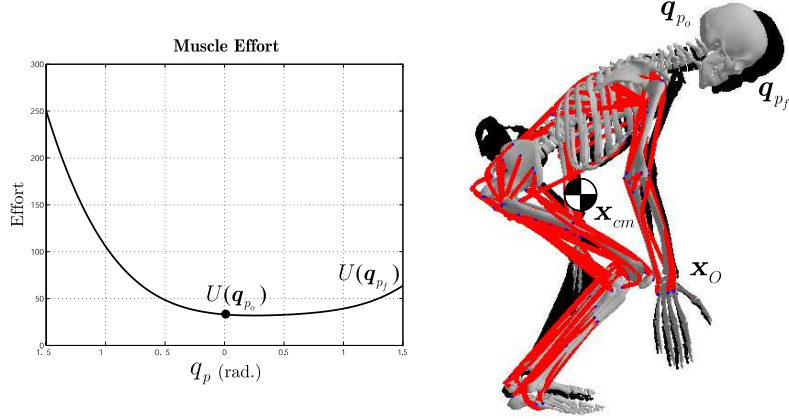


Figure 7. Plot showing muscle effort over null-space motion in whole body posture. Observed configuration, q_{p_o} , is 0.27 radians (15.5°) from the configuration where the computed minimum occurs.

The identification of this important postural behavior is encouraging for our research to map human motion behaviors for humanoid robot control. By using this potential to define the posture field U_p , we can utilize the posture space to minimize effort in real-time while performing any primary task \mathbf{x}_t . Moreover, the flexibility of our control framework will easily incorporate other behaviors upon identification. By establishing this basis, we expect to capture the characteristics that drive most of natural human motion.

5. Conclusions

Having constructed a dynamic musculoskeletal model of a human, we have proposed a methodology for identifying physiological characteristics and constraints that shape human motion. These characteristics are then mapped for robotic control by incorporating potentials into a prior-

itized task-level control framework. We investigated the muscular effort required for reaching tasks using this approach, and our analysis suggests that minimization of muscular effort is a vital objective of postural motion. By applying this methodology to other motion characteristics, we seek to incrementally construct a basis of human motion strategies.

6. Acknowledgements

The authors would like to acknowledge Scott Delp for his assistance and for providing musculoskeletal data. Additionally, the motion capture contributions of Chris Dyrby and Jaeheung Park are gratefully acknowledged.

References

- Anderson, F.C., and Pandy, M.G. (2001), Static and dynamic optimization solutions for gait are practically equivalent, *Journal of Biomechanics*, vol. 34, pp. 153–161.
- Crowninshield, R.D., and Brand, R.A. (1981), A physiologically based criterion of muscle force prediction in locomotion, *Journal of Biomechanics*, vol. 14, pp. 793–801.
- Delp, S., and Loan, P. (1995), A software system to develop and analyze models of musculoskeletal structures, *Computers in Biology and Medicine*, vol. 25, pp. 21–34.
- Hogan, N. (1991), Mechanical Impedance of Single- and Multi-Articular Systems. In *Multiple Muscle Systems*, New York, Springer Verlag.
- Ijspeert, A., Nakanishi, J., and Schaal, S. (2002), Movement imitation with nonlinear dynamical systems in humanoid robots, *Proceedings of the International Conference on Robotics and Automation*, pp. 1398–1403.
- Khatib, O. (1987), A unified approach to motion and force control of robot manipulators: The operational space formulation, *International Journal of Robotics Research*, vol. 3, no. 1, pp. 43–53.
- Khatib, O. (1995), Inertial properties in robotic manipulation: An object level framework, *International Journal of Robotics Research*, vol. 14, no. 1, pp. 19–36.
- Khatib, O., Brock, O., Chang, K-S., Conti, F., Ruspini, D., Sentis, L. (2002), Robotics and Interactive Simulation, *Communications of the ACM*, vol. 45, no. 3, pp. 46–51.
- Khatib, O., Sentis, L., Park, J., and Warren, J. (2004), Whole body dynamic behavior and control of human-like robots, *International Journal of Humanoid Robotics*.
- Kuroki, Y., Blank, B., Mikami, T., Mayeux, P., Miyamoto, A., Playter, R., Nagasaka, K., Raibert, M., Nagano, M., and Yamaguchi, J. (2003), Motion creating system for a small biped entertainment robot, *Proceedings of the International Conference on Intelligent Robots and Systems*, pp. 1394–1399.
- Schutte, L.M. (1992), *Using musculoskeletal models to explore strategies for improving performance in electrical stimulation-induced leg cycle ergometry*, PhD thesis, Stanford University.
- Zajac, F.E. (1993), Muscle coordination of movement: a perspective, *Journal of Biomechanics*, vol. 26, pp. 109–124.